Journal of Crystal Growth 395 (2014) 94–97

Contents lists available at ScienceDirect

Journal of Crystal Growth

journal homepage: www.elsevier.com/locate/jcrysgro

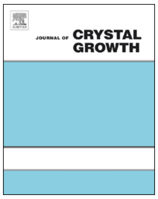

Czochralski growth of heavily tin-doped Si crystals

I. Yonenaga [a,*], T. Taishi [b], K. Inoue [a], R. Gotoh [a], K. Kutsukake [a], Y. Tokumoto [a], Y. Ohno [a]

[a] *Institute for Materials Research, Tohoku University, Sendai 980 8577, Japan*
[b] *Faculty of Engineering, Shinshu University, Nagano 380 8553, Japan*

ARTICLE INFO

Article history:
Received 16 October 2013
Received in revised form
13 February 2014
Accepted 14 February 2014
Communicated by A.G. Ostrogorsky
Available online 20 March 2014

Keywords:
A1. Doping
A1. Segregation
A1. Impurities
A1. Solubility
A2. Czochralski method
B2. Semiconducting silicon

ABSTRACT

Heavily tin (Sn)-doped Si crystals in a concentration up to $4\times10^{19}\ \text{cm}^{-3}$ were grown by the Czochralski method. Variation of Sn concentration in the crystals was well expressed by the Pfann equation using a segregation coefficient of $k=0.016$. From the occurrence of growth interface instability and the appearance of Sn precipitates in the grown crystals, the solubility limit of Sn was considered to be around $5\times10^{19}\ \text{cm}^{-3}$. Interstitially dissolved oxygen O_i was presented at a concentration of 8–$9\times10^{17}\ \text{cm}^{-3}$ in the grown Sn-doped crystals. The FT-IR absorption peak relating to a Si–O_i–Si quasi-molecule at $1106\ \text{cm}^{-1}$ showed preferential occupation of O_i at the bond-centered position of Si–Si. The O_i peak shifted to the lower wave number side with increasing Sn concentration in Si, implying expansion of the Si–Si bond.

1. Introduction

Recently isovalent impurities (Group-IV elements) have been attracting keen interest in the silicon (Si) industry. Such impurities have almost no effects on electrical properties, but their alloying with Si provides materials applicable in bandgap and lattice parameter engineering. Also, in doping cases they have unique interactions with harmful defects, resulting in improvement of the device yield and performance through local strain compensation. For example, germanium (Ge) is effective for suppression of the formation of quenched-in thermal donors [1] and electron-irradiation-induced vacancy-oxygen (VO) clusters in Czochralski-grown (CZ)-Si crystals [2–4]. Impurity tin (Sn) can be more effective in such defect suppression since the difference between its atomic size and the matrix Si is around 20%, larger than that of Ge, i.e., 4%. Indeed, Chroneos et al. reported inhibition or suppression of the formation of VO and VO_2 complexes in electron-irradiated Sn-rich CZ-Si [2–4]. Owing to this, Sn-doped CZ-Si is expected to replace Ge-doped CZ-Si due to its large strain effect in photovoltaic applications. For realizing applications, it is important to clarify fundamental properties of Si crystals doped with Sn at a variety of concentrations. However, there have been relatively few studies on the growth of heavily Sn-doped CZ-Si with the aim of characterizing Sn effects on oxygen-related defect generation [5–10]. Even now it is not entirely clear whether the solubility of Sn in Si is in the range of 7×10^{19} to $5\times10^{20}\ \text{cm}^{-3}$ in the phase diagram [11]. The segregation coefficient k is reported to be 0.016 [12]. That is, growth of heavily Sn-doped Si still needs to be elucidated.

Interstitially dissolved oxygen (O_i) is a peculiar impurity which occupies a bond-centered position and behaves as a Si–O_i–Si quasi-molecule, leading to local vibration centered at $1106\ \text{cm}^{-1}$ due to the ν_3 anti-symmetric stretching mode. In SiGe alloys, the Si–Si bond distance expands with incorporation of Ge into Si, resulting in a shift to the lower frequency of ν_3 [13,14]. Similarly, Sn is expected to have a remarkable effect on the vibration of O_i in Si due to the larger covalent radius of the Sn atom.

We attempted CZ-growth of Si crystals heavily doped with Sn in a concentration close to $10^{20}\ \text{cm}^{-3}$. We herein report the growth results and discuss variations of Sn concentration along the growth direction of the crystals and formation of grown-in defects. Doping effects of Sn on infrared absorption spectra of O_i are shown in terms of the dopant-induced elastic strain.

2. Experimental procedure

High-purity Si crystals (n-type: 5 Ωcm, ~60 g) were charged into a quartz crucible 50 mm in diameter and 50 mm in depth. Sn (5 N) rods were added to the crucible. [001]- or [111]-oriented Si crystals ~1 in. in diameter were grown by the CZ method at a pulling rate of 8 or 40 mm/h in a flowing gas atmosphere of high-purity Ar with a flux of 150 l/h under a pressure of 1 atm. The rotational rate of the crystal was 7.5 rpm, while that of the crucible

---

[*] Corresponding author. Tel.: +81 222152040; fax: +81 222152041.
E-mail address: yonenaga@imr.tohoku.ac.jp (I. Yonenaga).

http://dx.doi.org/10.1016/j.jcrysgro.2014.02.052

was 2 rpm in the opposite direction. Intentional Dash necking for dislocation-free crystal growth was not adopted. Detailed procedures and conditions of Si crystal growth have been described previously [15].

Grown crystals were cut into plates or blocks. The carrier concentration in square specimens $5 \times 5 \times 1\ \mathrm{mm}^3$ in size, prepared from various blocks, was determined by Hall-effect measurement using the van der Pauw method at room temperature (RT). The concentration of Sn impurity [Sn] was evaluated quantitatively by wave-length dispersive x-ray (WDX) spectroscopy using a JXA-8621MX (JEOL) and inductively coupled plasma-optical emission spectroscopy (ICP-OES). The concentration of interstitially dissolved oxygen [$\mathrm{O_i}$] in the grown crystals was measured at RT using a Fourier-transform infrared (FT-IR) spectrometer (JASCO FT-IR 610).

3. Results and discussion

3.1. Grown crystals

Two Si crystals doped with Sn in a concentration range up to $4 \times 10^{19}\ \mathrm{cm}^{-3}$ were grown. Table 1 summarizes the crystalline characteristics of the grown Sn-doped CZ-Si with various growth parameters.

Crystal #1, grown along the [111]-direction from a melt charged with 1.2 g of Sn, changed from single to polycrystalline in the latter half, as seen in Fig. 1(a). The main reason that polycrystallization was initiated may be that the adopted pulling rate was rather fast. Fig. 1(b) shows a boule of crystal #2 grown from a melt charged with 5 g of Sn. The boule was 70 mm in length and 25 mm in maximum diameter. It had four {111} facets on the outside of the body up to the tail, apparently showing that the boule was wholly single-crystalline with [001] growth direction. The crystal was n-type conductive and the carrier concentration estimated by the Hall-effect measurement was $6 \times 10^{14}\ \mathrm{cm}^{-3}$.

As seen in Table 1, [Sn] determined by WDX was at levels of 10^{18}–10^{19} and $10^{19}\ \mathrm{cm}^{-3}$ in grown crystals #1 and #2, respectively. Fig. 2 shows the variation of [Sn] against the solidification fraction g in crystal #2. [Sn] in the top region was around $1.5 \times 10^{19}\ \mathrm{cm}^{-3}$ and gradually increased along the growth direction to reach around $4 \times 10^{19}\ \mathrm{cm}^{-3}$ at the tail ($g \sim 0.62$). The variation of [Sn] is well reproduced by the Pfann equation [16], using $k = 0.016$, a segregation coefficient reported in the literature [12], as shown by a solid line superimposed in the figure.

The density of grown-in dislocations in crystal #2 was evaluated by the preferential etching method against the (001) cross-sectioned wafers with Sirtl etchant at RT [17]. The density was $3 \times 10^3\ \mathrm{cm}^{-2}$ in the top part and increased to $2 \times 10^4\ \mathrm{cm}^{-2}$ in the tail. Fig. 3 shows an optical micrograph of a wafer prepared from the tail part of the boule ($g \sim 0.62$). A number of etch-pit clusters can be seen in the micrograph. They were probably generated from precipitates of β-Sn [18]. In addition, cell structures exist around such etch pit clusters, as seen in Fig. 3. It should be noted that in crystal #1 grown at a higher pulling rate than crystal #2, polycrystallization occurred at the position of $g \sim 0.55$ where [Sn] was around $10^{19}\ \mathrm{cm}^{-3}$.

In the present growth studies, the occurrence of instability of the growth interface with precipitates and/or polycrystallization, strongly dependent on the pulling rate, was detected. This suggests that the concentration of Sn in the crystal part is rather close to the solubility limit in Si. That is, the solubility limit may be around $5 \times 10^{19}\ \mathrm{cm}^{-3}$, lower than that previously supposed [12]. It will be necessary to grow Sn-doped Si crystals under a much slower pulling rate for further clarification.

3.2. Oxygen impurity

Since the crystals were grown by the Czochralski method with a quartz crucible, a large number of interstitially dissolved oxygen atoms ($\mathrm{O_i}$) were included in the crystals. Fig. 4 shows infrared absorption spectra of Crystal #2 for various growth positions (fraction g) in the range of 800–1300 cm^{-1} at RT. A peak positioned at 1106 cm^{-1} was observed due to the local vibration of anti-symmetric stretching mode ν_3 of Si–$\mathrm{O_i}$–Si quasi-molecules. Here, Pomozov et al. reported the appearance of a few small

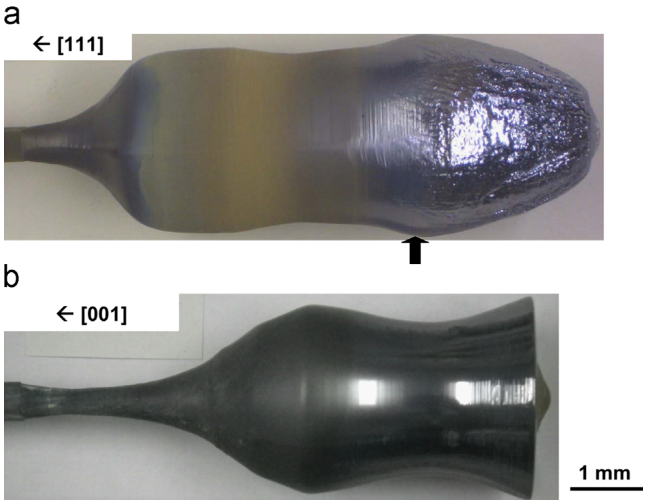

Fig. 1. Grown Si crystals heavily doped with Sn. (a) Crystal #1, (b) crystal #2. The arrow in (a) shows the position of the initiation of polycrystallization.

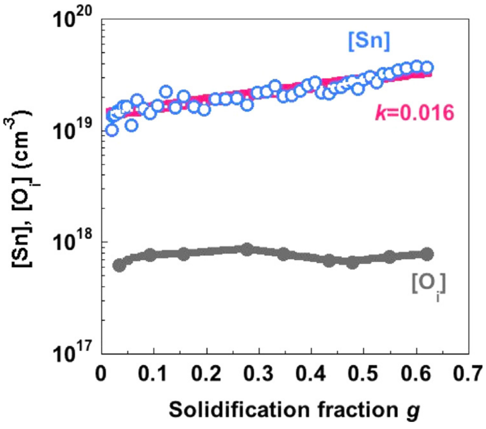

Fig. 2. Variation of concentrations of impurity tin [Sn] and interstitially dissolved oxygen [$\mathrm{O_i}$] against solidification fraction g in the Sn-doped Si crystals.

Table 1
Growth conditions for Sn-doped Si crystals and their crystalline characteristics. Concentrations of tin (Sn) and interstitially dissolved oxygen ($\mathrm{O_i}$) are also shown.

Crystal	Pulling direction	Pulling rate (mm/h)	[Sn] (cm^{-3})	[$\mathrm{O_i}$] (cm^{-3})	Remarks
#1	[111]	40	$4\text{–}30 \times 10^{18}$	8×10^{17}	Polycrystallization from the marked position
#2	[001]	10	$1.5\text{–}4 \times 10^{19}$	9×10^{17}	Development of cell structure and Sn precipitates